GSA Data Repository Item 2019158

Dean, D.J., and Topping, D.J., 2019, Geomorphic change and biogeomorphic feedbacks in a dryland river: The Little Colorado River, Arizona, USA: GSA Bulletin, https://doi.org/10.1130/B35047.1.

Data Repository

Figure DR1. 1923-2016 repeat photographs of the LCR at Cameron, AZ.

Figure DR2. Image of the Lyman Lake Dam following the dam break in 1915. Image obtained from http://web.sahra.arizona.edu/education2/wrtt/lecs/Johnson_P2_DamFailures_ho.pdf.

Figure DR3. Aerial-photograph maps of the *above Cameron*, *Cameron to Moenkopi*, and *below Moenkopi* reaches (a), *Black Falls* reach (b), and *Grand Falls* reaches (c). Images were taken in 2013 by the National Aerial Imagery Program.

Figure DR4. Topographic measurements made at the Grand Falls cableway cross section depicting seasonal scour and fill in 1929 and 1930. Elevations are orthometric heights above the 1983 North American Datum, calculated using GEOID 12a.

Figure DR5. Minimum bed elevation observed during discharge measurements at the Grand Falls and near Cameron Gages. High and low flow periods refer to periods of high and low TAF in Hydrology Results section and are depicted by gray dashed lines.

Figure DR6. Discharge — suspended-silt-and-clay concentration relations at the *at* Cameron gage (a and b) and the *near* Cameron gage (c and d). Summer/fall season relations for suspended silt and clay are shown in (a) and (c). Winter/spring season relations for suspended silt and clay are shown in (b) and (d).

Figure DR7 (previous page). Repeated cross sections in the *above Grand Falls* reach, from upstream (a) to downstream (d). Within original 1940 survey, cross sections were labeled as D, C, B, A, A', from upstream to downstream. Thus, here, cross section D is shown in (a), cross section B is shown in (b), cross section A is shown in (c), and cross section A' is shown in (d). Cross section C is presented in Figure 7c. Elevations are orthometric heights above the 1983 North American Datum, calculated using GEOID 12a. The local 1940 coordinates have been translated accordingly.

Figure DR8 (this page and previous two pages). Repeated cross sections in the *above Cameron* reach from upstream (a) to downstream (i). Cross sections (a) – (h) represent the first 8 cross sections, and (i) represents the 10^{th} cross section downstream. The 9^{th} cross section is depicted in

Figure 7d. Elevations are orthometric heights above the 1983 North American Datum, calculated using GEOID 12a.

Figure DR9. Repeat photograph of LCR above Cameron, AZ. Photo (a) depicts the LCR in October 21, 1964 looking downstream. Photo (b) depicts the LCR on December 13, 2016. Photo (a) was taken by unknown photographer of the USGS, and photo (b) was taken by the authors. Note that the low bridge in the middle of the photo was removed in 2016 prior to the date photo (b) was collected.

Figure DR10. Channel cross section surveys at the former bridge crossing above Cameron, AZ. Note that when the bridge was removed, the abutments were also removed resulting in less vertical banks during the 2016 survey. Elevations from 1983 are likely within about 0.5 m, as the elevations were measured down from the bridge railing, and the exact elevation of the bridge and its railing were unknown during the 2016 survey because the bridge had been removed.

Figure DR11. Photograph of the LCR looking downstream in the *Cameron to Moenkopi* reach showing the dominant vegetation types of tamarisk and willow. Photograph taken by D.J. Dean on May 19, 2016.

Figure DR12. Annual precipitation data for Winslow, AZ (a), Springerville, AZ (b), and the number of days with greater than 2.54 cm of rain at Winslow (c), Springerville (d). Annual data are diamonds, horizonal lines are averages for the four time periods identified in the Hydrology Results section, and dark wavy lines are 5-year running averages. Data were obtained from https://www.ncdc.noaa.gov/cdo-web/datatools/. Missing data was obtained from Sellers and Hill (1974).

Table DR1. Sediment Sampling Locations

Table DR2. AERIAL PHOTOGRAPH SOURCES

Table DR3. ERRORS ASSCIATED WITH CHANNEL WIDTH MEASUREMENTS ON AERIAL PHOTOGRAPHS

Table DR4. HYDRAULIC MODELING PARAMETERS

Table DR5. HYDRAULIC MODELING INPUTS

Table DR6. CHANNEL WIDTH MEASUREMENTS DETERMINTED FROM AERIAL PHOTOGRAPH ANALYSIS

Table DR7. RESULTS OF THE REGRESSION ANALYSES FOR DISCHARGE—CONCENTRATION RELATIONS

Table DR8. RESULTS OF HYDRAULIC MODELING

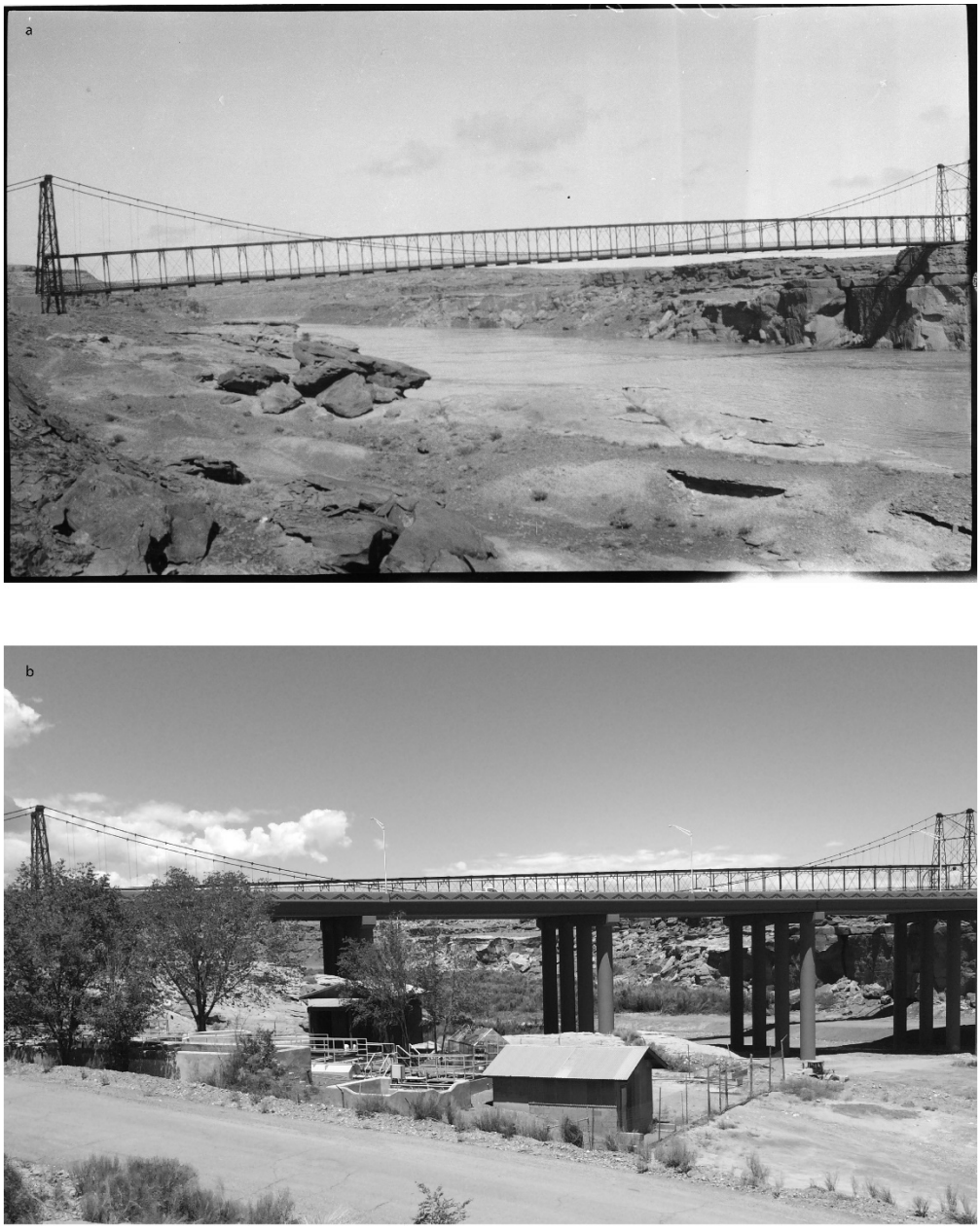

Figure DR1. 1923-2016 repeat photographs of the LCR at Cameron, AZ. Photo (a) depicts the LCR during a flood with an estimated peak discharge of ~3,400 m^3/s (i.e. 120,000 ft^3/s) at 9:40 a.m. on September 19, 1923; photo taken by G.C. Stevens of the USGS on the left side of the LCR, looking downstream. The photograph in (a) was likely taken near peak discharge of this flood. Repeat photograph in (b) taken by D.J. Dean on May 19, 2016. A second bridge that now serves as Highway 89 has been built upstream of the original suspension bridge in (a). The discharge of this flood was estimated on the basis of rating-curve extrapolation at the Grand Falls gage in combination with analysis of the records from gaging stations on the Colorado River that bracket the LCR. Measurements made on December 13, 2016 indicate that the stage of the 1923 flood in (a) was approximately 6 m above the bed of the river in (b).

Figure DR2. Image of the Lyman Lake Dam following the dam break in 1915. Image obtained from http://web.sahra.arizona.edu/education2/wrtt/lecs/Johnson_P2_DamFailures_ho.pdf.

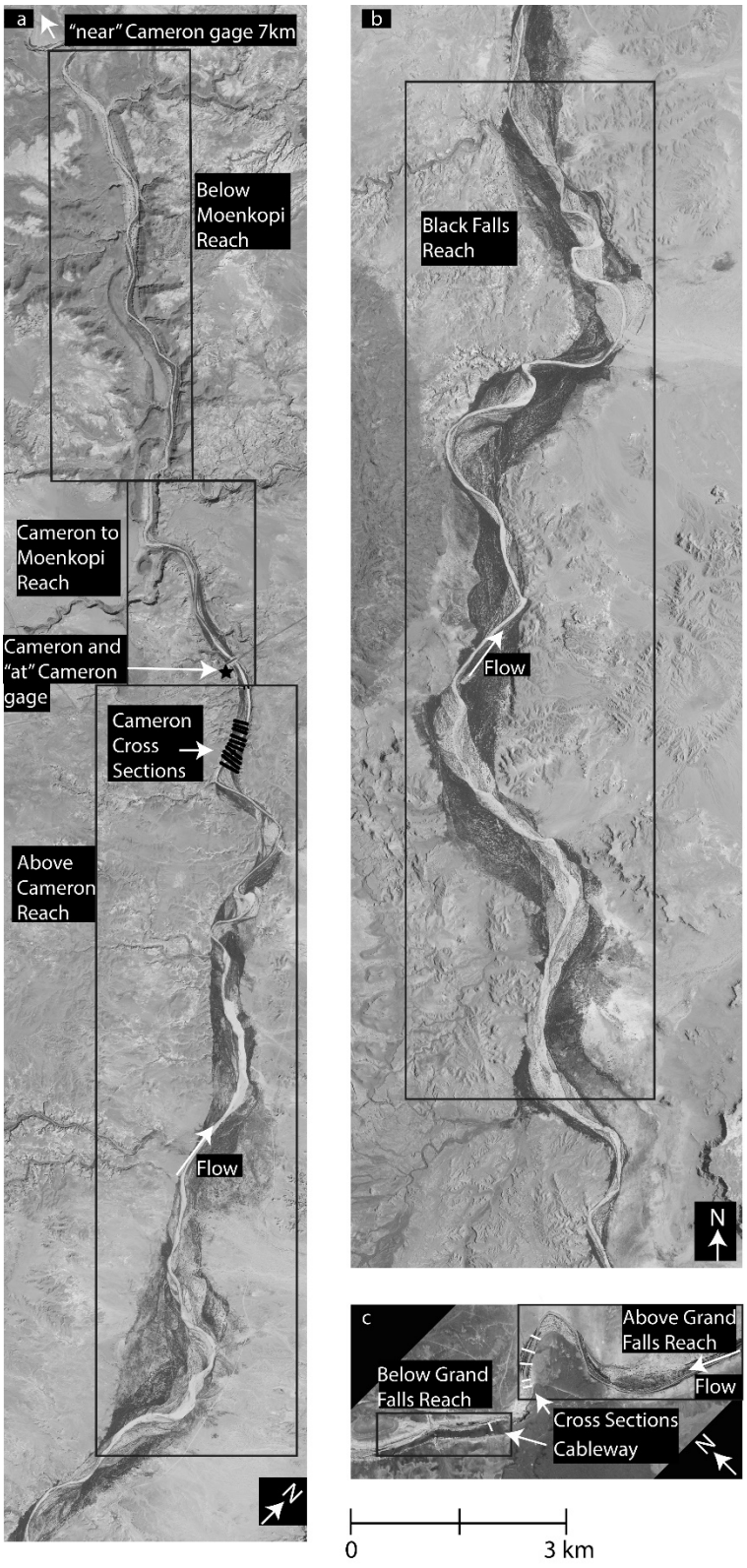

Figure DR3. Aerial-photograph maps of the *above Cameron*, *Cameron to Moenkopi*, and *below Moenkopi* reaches (a), *Black Falls* reach (b), and *Grand Falls* reaches (c). Images were taken in 2013 by the National Aerial Imagery Program.

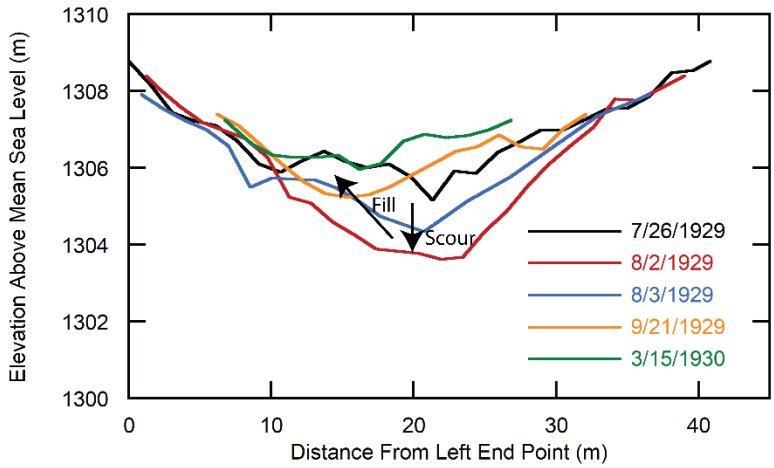

Figure DR4. Topographic measurements made at the Grand Falls cableway cross section depicting seasonal scour and fill in 1929 and 1930. Elevations are orthometric heights above the 1983 North American Datum, calculated using GEOID 12a.

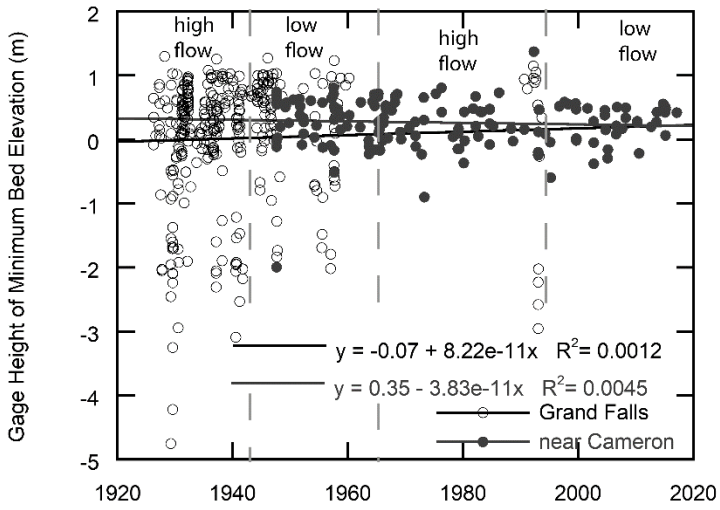

Figure DR5. Minimum bed elevation observed during discharge measurements at the Grand Falls and near Cameron Gages. High and low flow periods refer to periods of high and low TAF in Hydrology Results section and are depicted by gray dashed lines.

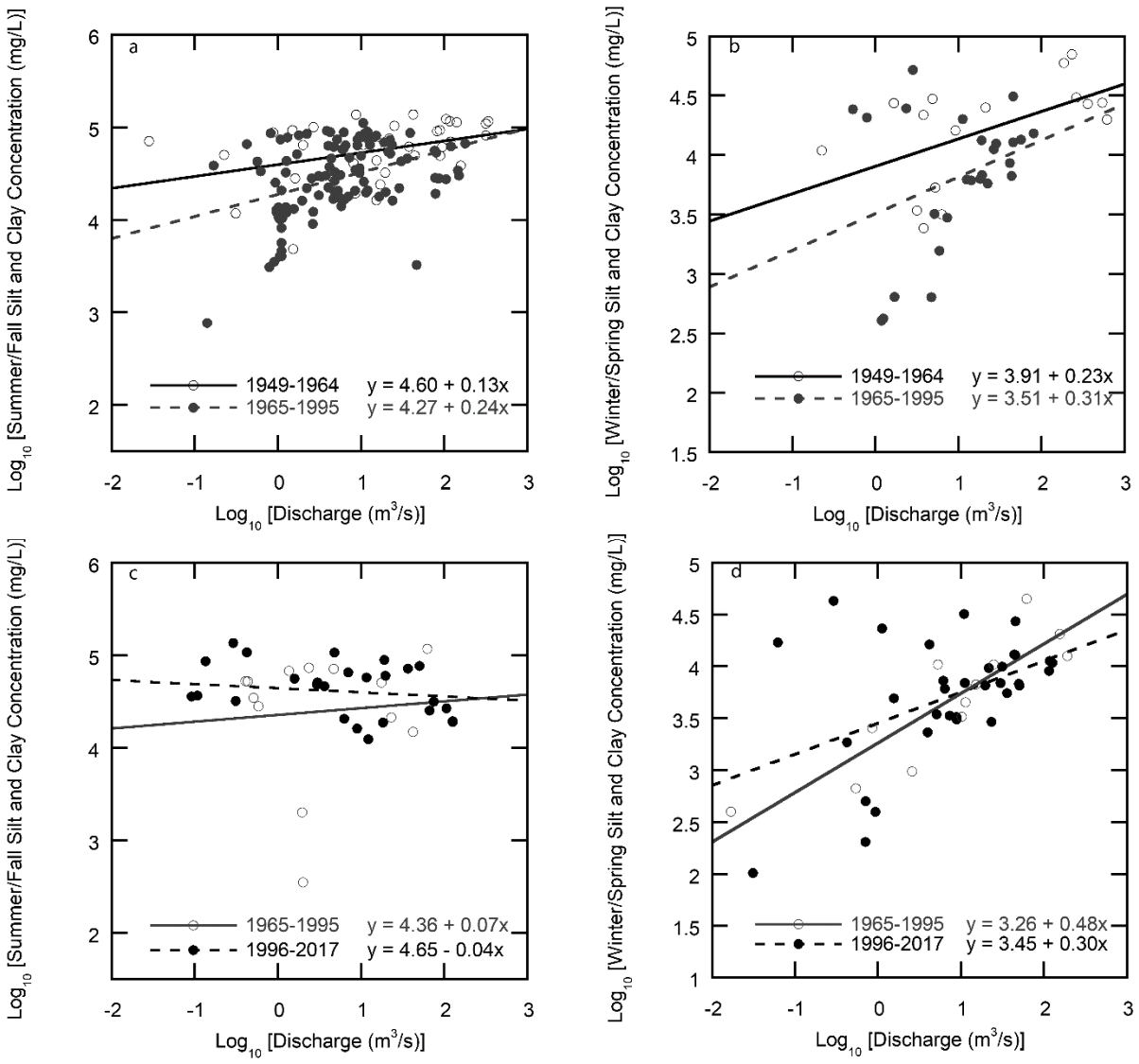

Figure DR6. Discharge — suspended-silt-and-clay concentration relations at the *at* Cameron gage (a and b) and the *near* Cameron gage (c and d). Summer/fall season relations for suspended silt and clay are shown in (a) and (c). Winter/spring season relations for suspended silt and clay are shown in (b) and (d).

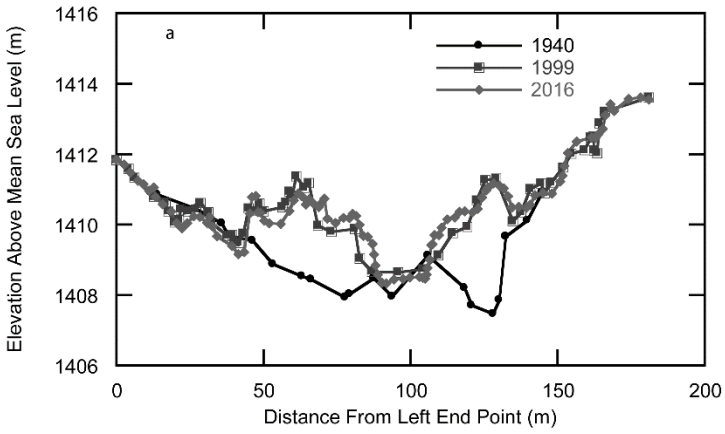
a
1940
1999
2016
Elevation Above Mean Sea Level (m)
1416
1414
1412
1410
1408
1406
0
50
100
150
200
Distance From Left End Point (m)

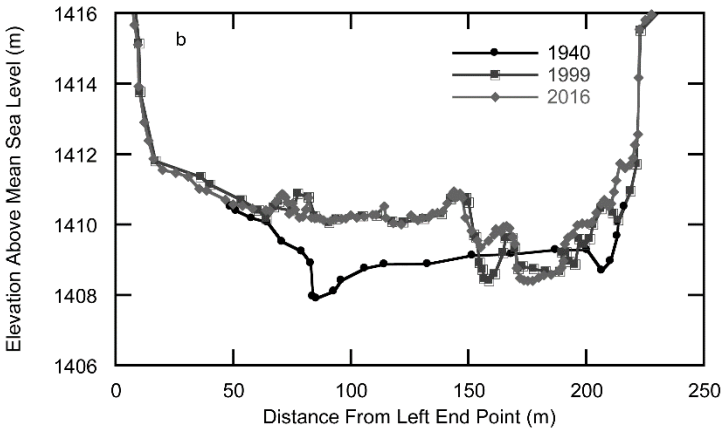
b
1940
1999
2016
Elevation Above Mean Sea Level (m)
1416
1414
1412
1410
1408
1406
0
50
100
150
200
250
Distance From Left End Point (m)

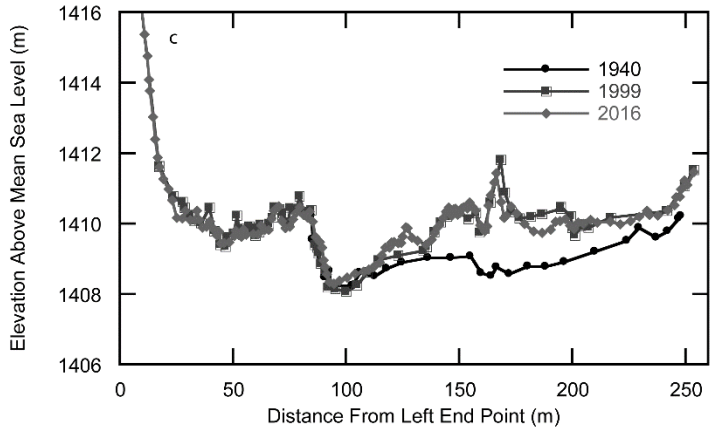
c
1940
1999
2016
Elevation Above Mean Sea Level (m)
1416
1414
1412
1410
1408
1406
0
50
100
150
200
250
Distance From Left End Point (m)

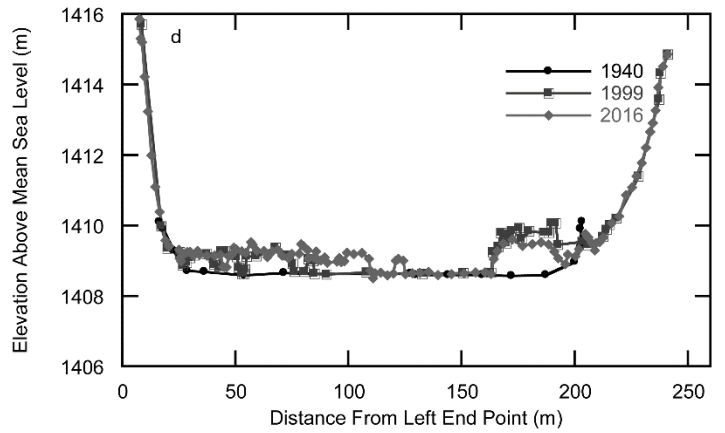
d
1940
1999
2016
Elevation Above Mean Sea Level (m)
1416
1414
1412
1410
1408
1406
0
50
100
150
200
250
Distance From Left End Point (m)

Figure DR7 (previous page). Repeated cross sections in the *above Grand Falls* reach, from upstream (a) to downstream (d). Within original 1940 survey, cross sections were labeled as D, C, B, A, A', from upstream to downstream. Thus, here, cross section D is shown in (a), cross section B is shown in (b), cross section A is shown in (c), and cross section A' is shown in (d). Cross section C is presented in Figure 7c. Elevations are orthometric heights above the 1983 North American Datum, calculated using GEOID 12a. The local 1940 coordinates have been translated accordingly.

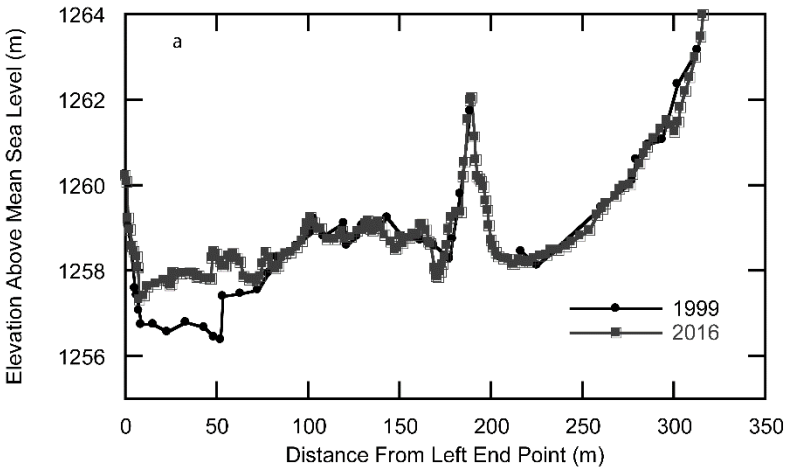
a
Elevation Above Mean Sea Level (m)
1264
1262
1260
1258
1256
0
50
100
150
200
250
300
350
Distance From Left End Point (m)
1999
2016

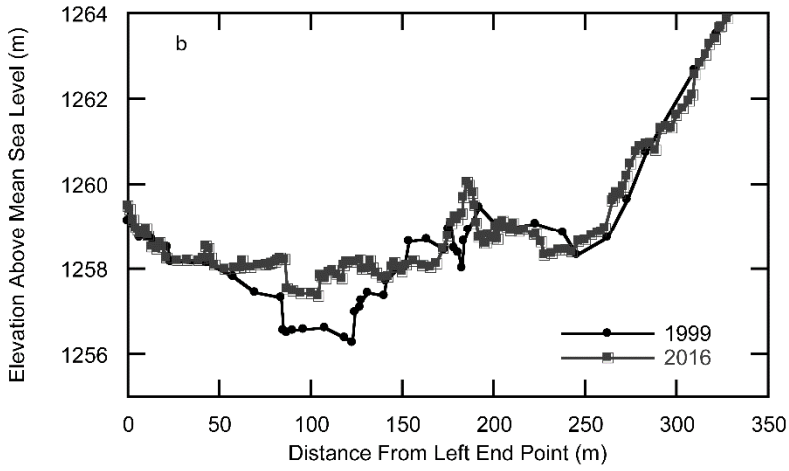
b
Elevation Above Mean Sea Level (m)
1264
1262
1260
1258
1256
0
50
100
150
200
250
300
350
Distance From Left End Point (m)
1999
2016

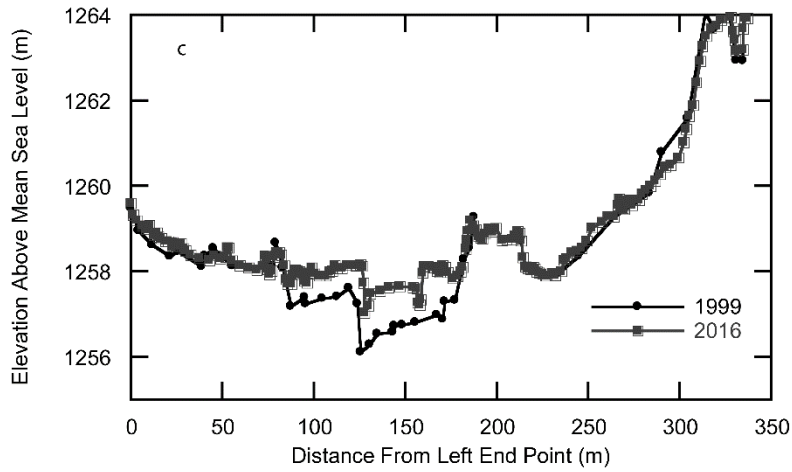
c
Elevation Above Mean Sea Level (m)
1264
1262
1260
1258
1256
0
50
100
150
200
250
300
350
Distance From Left End Point (m)
1999
2016

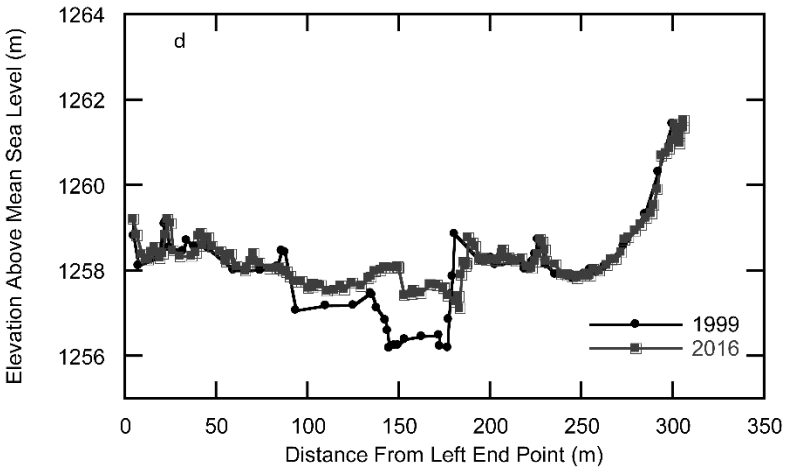
d
1999
2016
Elevation Above Mean Sea Level (m)
Distance From Left End Point (m)
1264
1262
1260
1258
1256
0
50
100
150
200
250
300
350

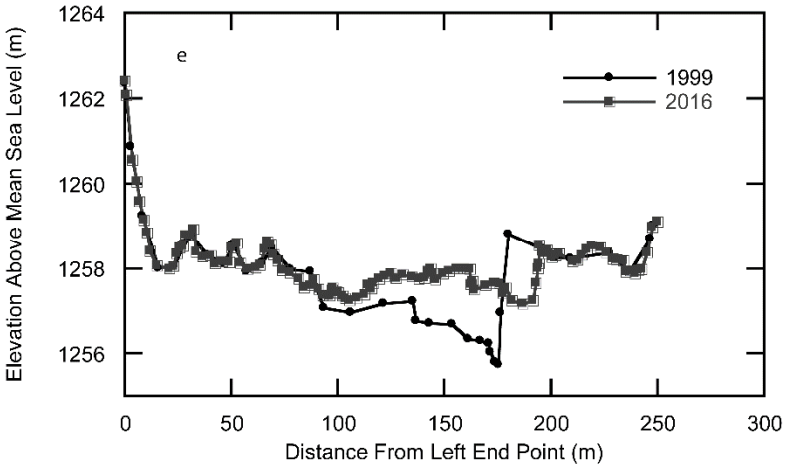
e
1999
2016
Elevation Above Mean Sea Level (m)
Distance From Left End Point (m)
1264
1262
1260
1258
1256
0
50
100
150
200
250
300

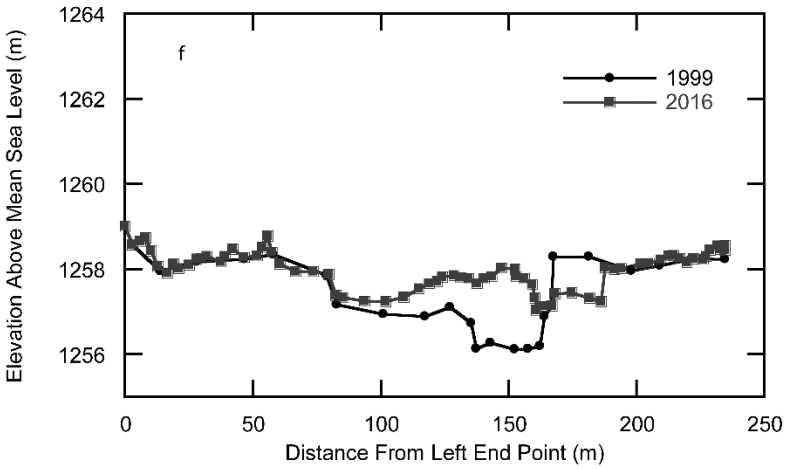
f
1999
2016
Elevation Above Mean Sea Level (m)
Distance From Left End Point (m)
1264
1262
1260
1258
1256
0
50
100
150
200
250

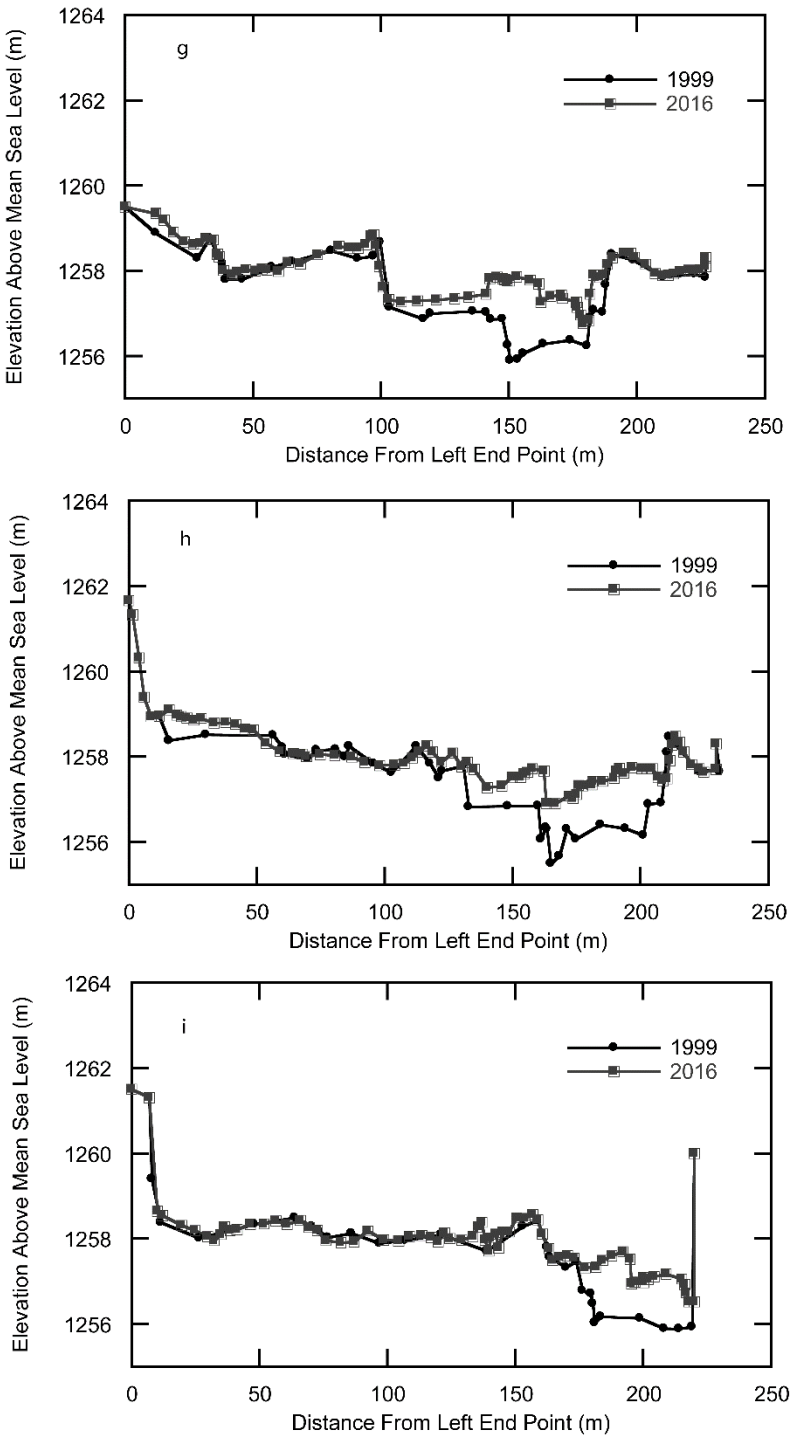

Figure DR8 (this page and previous two pages). Repeated cross sections in the *above Cameron* reach from upstream (a) to downstream (i). Cross sections (a) – (h) represent the first 8 cross sections, and (i) represents the 10th cross section downstream. The 9th cross section is depicted in Figure 7d. Elevations are orthometric heights above the 1983 North American Datum, calculated using GEOID 12a.

Figure DR9. Repeat photograph of LCR above Cameron, AZ. Photo (a) depicts the LCR in October 21, 1964 looking downstream. Photo (b) depicts the LCR on December 13, 2016. Photo (a) was taken by unknown photographer of the USGS, and photo (b) was taken by the authors. Note that the low bridge in the middle of the photo was removed in 2016 prior to the date photo (b) was collected.

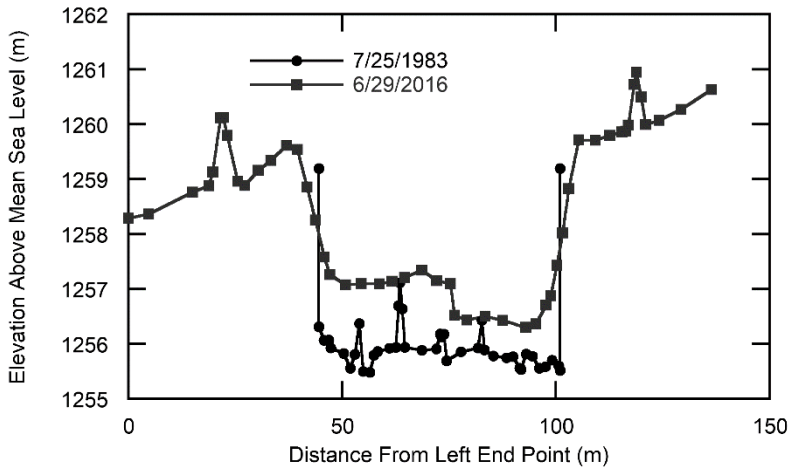

Figure DR10. Channel cross section surveys at the former bridge crossing above Cameron, AZ. Note that when the bridge was removed, the abutments were also removed resulting in less vertical banks during the 2016 survey. Elevations from 1983 are likely within about 0.5 m, as the elevations were measured down from the bridge railing, and the exact elevation of the bridge and its railing were unknown during the 2016 survey because the bridge had been removed.

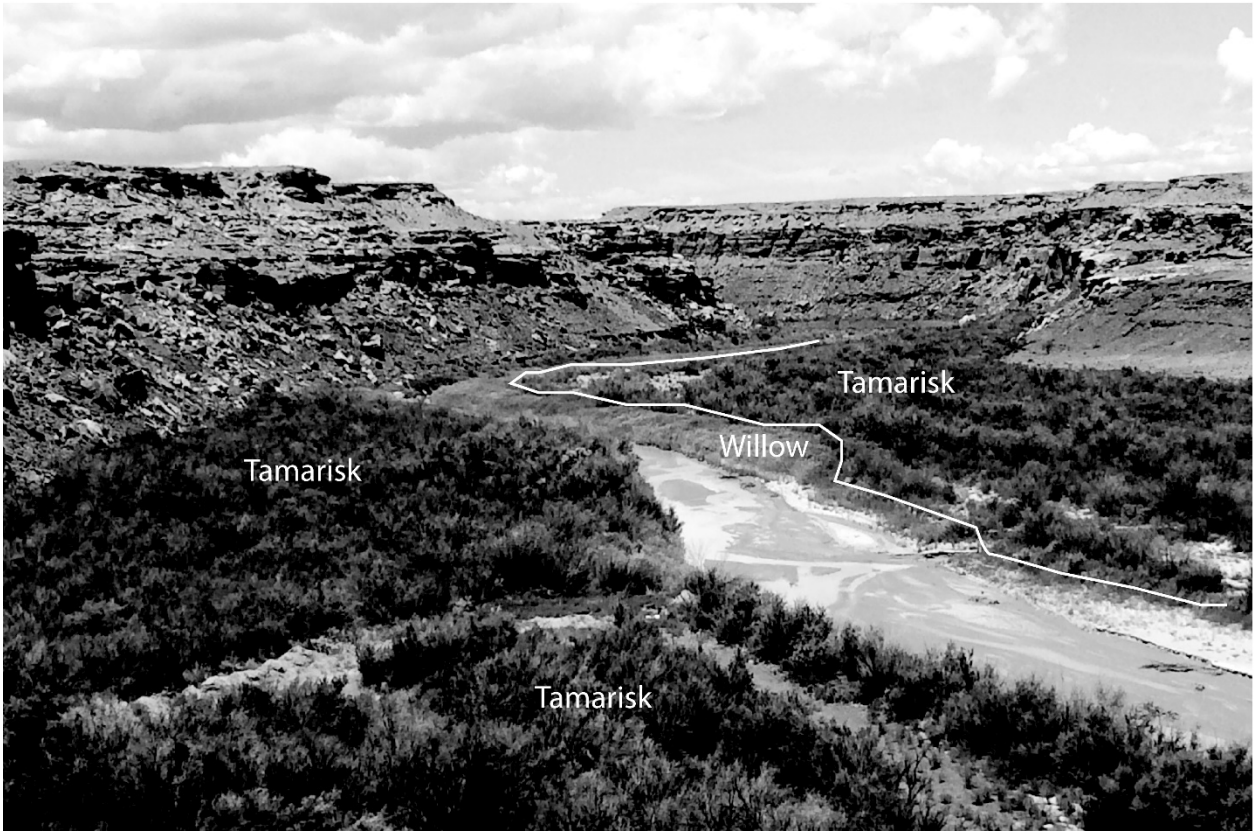

Figure DR11. Photograph of the LCR looking downstream in the *Cameron to Moenkopi* reach showing the dominant vegetation types of tamarisk and willow. Photograph taken by D.J. Dean on May 19, 2016.

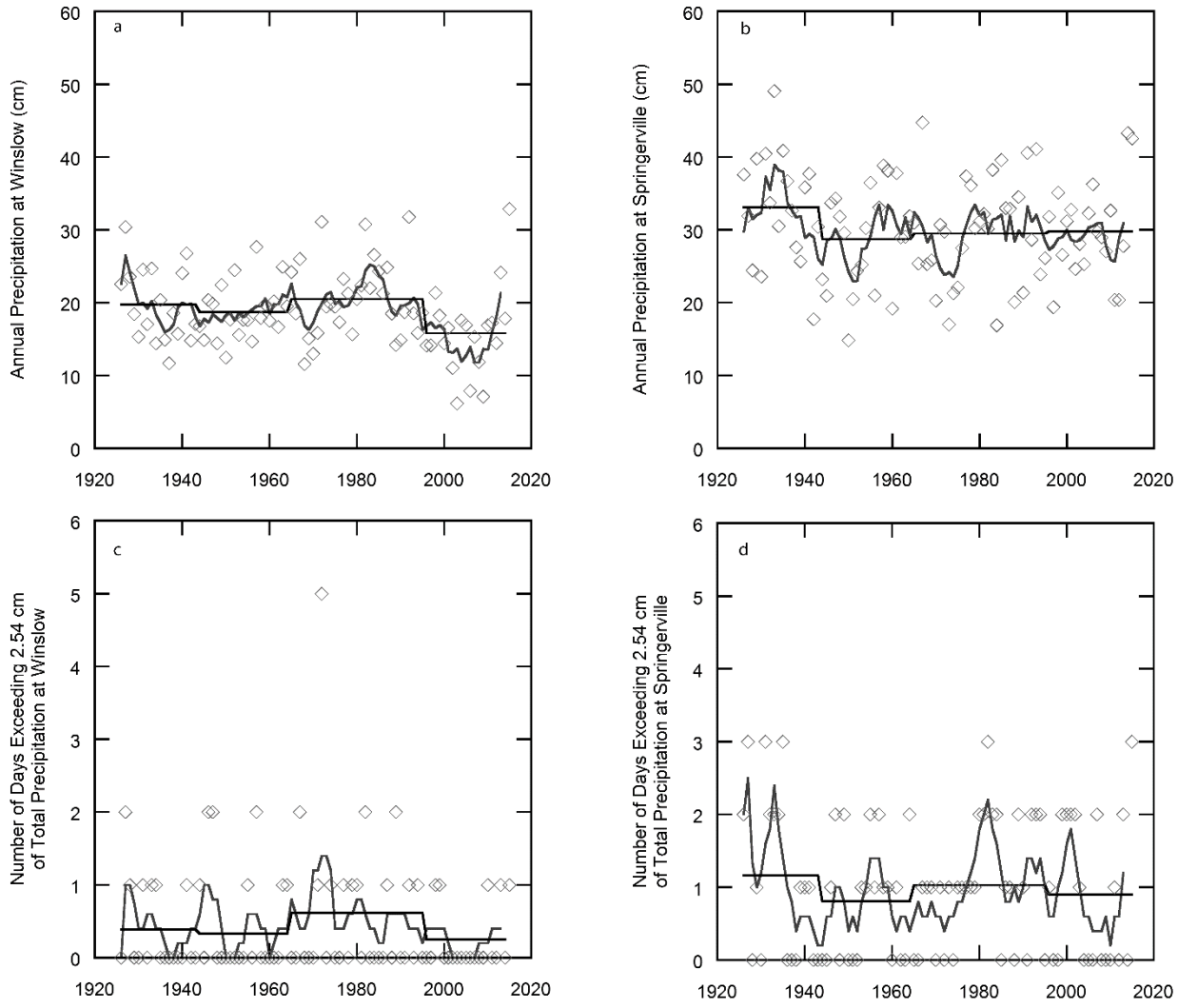

Figure DR12. Annual precipitation data for Winslow, AZ (a), Springerville, AZ (b), and the number of days with greater than 2.54 cm of rain at Winslow (c), Springerville (d). Annual data are diamonds, horizonal lines are averages for the four time periods identified in the Hydrology Results section, and dark wavy lines are 5-year running averages. Data were obtained from https://www.ncdc.noaa.gov/cdo-web/datatools/. Missing data was obtained from Sellers and Hill (1974).

Sellers, W.D., Hill, R.H. (Eds.), 1974. Arizona climate, 1931-1972. Tuscon, AZ, University of Arizona Press.

Table DR1. Sediment Sampling Locations

Location	Time period of Sampling
Little Colorado River at Grand Falls, AZ (station #09401000)	1931, 1990-1994, 2002-2014
Little Colorado River *at* Cameron, AZ (station #09401200)	1947-1970, 1974-1986, 1994-2000
Little Colorado River *near* Cameron, AZ (station #09402000)	1957-1958, 1966-1970, 1994-present
Little Colorado River above the mouth near Desert View, AZ (station #09402300)	1983, 1991-1993, 1998, 2003-present

Table DR2. AERIAL PHOTOGRAPH SOURCES

Digital scans of the 1930s imagery were obtained from the National Archives and Records Administration, and scans of the later imagery were obtained from the USGS Earth Resources Observation and Science Center. Scans were obtained at the highest possible resolution. Digital imagery taken in 2007, 2010, and 2013 were orthorectified by the National Aerial Imagery Program (NAIP). Digital scans for the previous years were orthorectified by Pinnacle Mapping Technologies in Flagstaff, AZ, using photogrammetric block calibration in ERDAS IMAGINE. The reported Root Mean Square Errors (RMSEs) for orthorectification are reported in Table DR3.

Year	Source	Obtained from
1933-1934	U.S. Soil Conservation Service	NARA[*]
1936	U.S. Soil Conservation Service	NARA
1952-1954	U.S. Army Map Service	USGS EROS[†]
1968	U.S. Geological Survey	USGS EROS
1979	U.S. Geological Survey	USGS EROS
1992	National Aerial Photography Program	USGS EROS
1997	National Aerial Photography Program	USGS EROS
2007	National Agricultural Imagery Program	USGS EROS
2010	National Agricultural Imagery Program	USGS EROS
2013	National Agricultural Imagery Program	USGS EROS

[*]U.S. National Archives and Records Administration

[†]U.S. Geological Survey Earth Resources Observation and Science Center

Table DR3. ERRORS ASSCIATED WITH CHANNEL WIDTH MEASUREMENTS ON AERIAL PHOTOGRAPHS

Uncertainty in the delineation of the active-channel boundaries were evaluated using the methods of Mount et al. (2003) and Swanson et al. (2011) where the error in active-channel width delineation (E_ω) is defined as follows:

$$\mathrm{E}_\omega = \sqrt{2\rho\mathrm{R}} + 2\Theta, \quad (1)$$

where $\sqrt{2\rho\mathrm{R}}$ is the error associated with digitizing the bank lines, and 2Θ is the image distortion error. Here, ρ is the mean width between repeat bank-line digitizations in meters and R is pixel resolution in m/pixel. For each year of aerial imagery, we calculated ρ by digitizing the left and right bank of a 5 km section of the *above Cameron* reach, 5 times each, and then calculated the mean distance of each line from the digitized active-channel boundary; the *above Cameron* reach is the reach with the greatest geomorphic complexity. During this process, we made sure to digitize the boundaries of all channel-margin features where there was uncertainty in the original active-channel delineation. In 1968, there was insufficient aerial photograph coverage of the *above Cameron* reach, therefore, we calculated ρ using a 5 km section of the *Black Falls* reach. In 1952, there were only photographs of the *above* and *below Grand Falls* reaches, therefore we calculated ρ using a 5km section of the those two reaches that spanned both upstream and downstream of the falls. The image distortion error 2Θ was evaluated as 2 times the RMSE, or the reported uncertainty in the ground sample distance compared to the true ground distance reported for the NAIP imagery.

Date	Reaches[*]	Width error ρ	Scan Resolution *R* (m/pixel)	Digitization Error √(2ρR), (m)	RMSE (pixels)	Θ (m)	Total Error E_ω (m)
1933-1934[†]	Cameron[§]	6.46	0.40	2.27	0.10	0.04	2.35
10/7/1936	Black Falls	6.46	0.90	3.41	0.10	0.09	3.59
1933-1934[†]	Grand Falls[#]	6.46	0.50	2.54	2.80	1.40	5.34
9/11/1953, 4/1/1954	Cameron	2.61	1.00	2.28	1.31	1.31	4.90
4/1/1954	Black Falls	2.61	1.00	2.28	1.46	1.46	5.20
10/10/1952, 10/23/1952	Grand Falls	4.20	0.60	2.24	0.95	0.57	3.38
	Cameron	N.A.	N.A.	N.A.	N.A.	N.A.	N.A.
6/1, 6/13, 9/1/1968	Black Falls	2.32	0.70	1.80	1.22	0.85	3.51
6/13/1968	Grand Falls	2.32	0.70	1.80	1.03	0.72	3.24
4/19-20/1979,	Cameron	1.75	0.71	1.58	1.35	0.96	3.49
4/20-21, 8/22/1979	Black Falls	1.75	0.70	1.56	1.01	0.71	2.98
4/19, 8/22/1979	Grand Falls	1.75	0.70	1.56	1.18	0.83	3.22
4/17, 9/1/1992	Cameron	2.55	0.30	1.24	1.45	0.44	2.11
4/17/1992	Black Falls	2.55	1.00	2.26	1.48	1.48	5.22
4/17, 9/22/1992	Grand Falls	2.55	0.30	1.24	1.12	0.34	1.91
7/4, 7/7, 10/17,1997	Cameron[**]	5.77	1.00	3.40	1.69	1.69	6.77
7/4, 7/7, 10/17,1997	Black Falls[**]	6.81	0.30	2.02	2.42	0.73	3.47
10/16-17,1997	Grand Falls[**]	5.77	0.30	1.86	2.20	0.66	3.18

6/8/2007	Cameron[†]	1.86	1.00	1.93	N.A.	6.00	13.93
6/8/2007	Black Falls[†]	1.86	1.00	1.93	N.A.	6.00	13.93
6/1, 6/8/2007	Grand Falls[†]	1.86	1.00	1.93	N.A.	6.00	13.93
6/5/2010	Cameron[†]	2.16	1.00	2.08	N.A.	6.00	14.08
6/5/2010	Black Falls[†]	2.16	1.00	2.08	N.A.	6.00	14.08
7/27/2010	Grand Falls[†]	2.16	1.00	2.08	N.A.	6.00	14.08
6/7, 6/18-19/2013	Cameron[†]	2.93	1.00	2.42	N.A.	6.00	14.42
6/18-19/2013	Black Falls[†]	2.93	1.00	2.42	N.A.	6.00	14.42
6/18/2013	Grand Falls[†]	2.93	1.00	2.42	N.A.	6.00	14.42

[*]Given that the three downstream reaches near Cameron, and the two upstream reaches near Grand Falls are contiguous, these reaches are grouped under "Cameron" and "Grand Falls" reaches, respectively, to conserve space

[†]Exact air photo dates unknown. Photo set known to pre-date a meander cutoff near a USGS gaging station on Moenkopi Wash that occurred on August 28, 1934

[§]No coverage for Cameron to Moenkopi reach, or below Moenkopi reach.

[#]Coverage only exists for the above Grand Falls reach.

[**]Digital orthophoto quarter quadrangles available for download from USGS EROS, RMSE is average of reported RMSE for each quarter quadrangle.

[##]No RMSE for these digital orthophoto quadranges reported, Θ is the reported error between ground sample distance to true ground.

Table DR4. HYDRAULIC MODELING PARAMETERS

1-Dimensional hydraulic modeling was conducted using U.S. Army Corps of Engineers Hydrologic Engineering Center's River Analysis System (HEC-RAS). A Simplified channel geometry was created by using the average values of reach-averaged channel widths measured on aerial photographs in 1953/1954 and 2013 (Table DR6), and an estimated channel depth of 2m, with 45 degree banks, thus creating a trapezoidal channel. The width of the alluvial valley was also approximated at 750 m based on the alluvial widths in Table 1. Channel slopes and Manning's n roughness values of the first two runs were based on a historical channel survey conducted in the *above Grand Falls* reach in 1940 (Fig. 4c). Water surface slopes from that survey ranged between 0.00066 and 0.0014, and Manning's n was estimated to be between 0.018 and 0.022. We chose an initial model slope of 0.0008 which more closely resembles the water surface slope at the upstream end of the survey reach (see cross sections Fig. DR7a and b) before the water surface begins steepening as it approaches Grand Falls. We used a channel roughness of 0.018 and a floodplain roughness of 0.02 in model runs 1-3. In model run 4, floodplain roughness was increased to 0.1, which is a reasonable approximation based on the density of the floodplain forests (Fig. 4b).

Model Run/ Simulation Year	Alluvial Valley Width (m)	Channel Width (m)	Channel Depth (m)	Slope	Channel Length (km)	Cross Section Spacing (m)	Manning's n Channel	Manning's n Floodplain
1 - 1954	750	350	2	0.0008	36	100	0.018	0.02
2 - 2013	750	62	2	0.0008	36	100	0.018	0.02
3 - 2013	750	62	2	0.00071	40.5	100	0.018	0.02
4 - 2013	750	62	2	0.00071	40.5	100	0.018	0.1

Table DR5. HYDRAULIC MODELING INPUTS

The input hydrograph consisted of the streamflow measured at the Grand Falls gage between 3/25/1954 and 3/30/1954. The rise of the input hydrograph was modified to improve model stability and convergence, and discharge values were linearly interpolated to 15-minute timestamps for the model input. The model was run from 3/24/1954 18:45 through 3/29/1954 at 00:00. The Input hydrograph can be downloaded at *https://doi.org/10.5066/P9XPWIBM* (Dean and Topping, 2018). Channel geometry data are listed below.

1954		2013	
Distance from Left End Point (m)	Elevation (m)	Distance from Left End Point (m)	Elevation (m)
0	100	0	100
0	90	0	90
200	90	344	90
202	89	346	89
548	89	404	89
550	90	406	90
750	90	750	90
750	100	750	100

TABLE DR6. CHANNEL WIDTH MEASUREMENTS DETERMINTED FROM AERIAL PHOTOGRAPH ANALYSIS

	Above Cameron		Cameron to Meonkopi Wash		Below Moenkopi		Black Falls		Above Grand Falls		Below Grand Falls	
Year	Active-channel width (m)	% of channel width of first photograph	Active-channel width (m)	% of channel width of first photograph	Active-channel width (m)	% of channel width of first photograph	Active-channel width (m)	% of channel width of first photograph	Active-channel width (m)	% of channel width of first photograph	Active-channel width (m)	% of channel width of first photograph
1933/34	495.9	100.0	136.3	100	N.A.	N.A.	N.A.	N.A.	176.6	100.0	N.A.	N.A.
1936	N.A.	N.A.	N.A.	N.A.	N.A.	N.A.	412.8	100.0	N.A.	N.A.	N.A.	N.A.
1952	N.A.	N.A.	N.A.	N.A.	N.A.	N.A.	N.A.	N.A.	131.4	74.4	47.3	100.0
1954	358.1	72.2	122.1	89.6	71.1	100.0	334.2	81.0	N.A.	N.A.	N.A.	—
1968	N.A.	N.A.	N.A.	N.A.	N.A.	N.A.	251.1	60.8	56.6	32.0	46.7	98.8
1979	252.3	50.9	86.2	63.3	62.8	88.3	286.2	69.3	44.2	25.0	48.0	101.5
1992	150.1	30.3	66.2	48.6	43.9	61.7	129.4	31.3	35.8	20.3	45.5	96.2
1997	111.6	22.5	55.8	41.0	49.9	70.2	124.0	30.0	30.7	17.4	41.5	87.7
2007	101.8	20.5	44.3	32.5	40.2	56.5	75.8	18.4	24.4	13.8	34.4	72.8
2010	82.8	16.7	41.1	30.2	35.5	49.9	72.1	17.5	22.3	12.6	35.2	74.4
2013	66.9	13.5	37.5	27.5	35.1	49.4	56.3	13.6	21.1	11.9	37.5	79.3

TABLE DR7: RESULTS OF THE REGRESSION ANALYSES FOR DISCHARGE—CONCENTRATION RELATIONS

Periods	Sediment fraction	Season	Intercept 1st period	Slope 1st period	Standard error	Intercept 1st period log transformed	Slope 1st period log transformed	Standard error log transformed	Intercept 2nd period	Slope 2nd period	Standard error	Intercept 2nd period log transformed	Slope 2st period log transformed	Standard error log transformed	Significant at alpha p=0.05?	F value	p value
1949-1964/	Silt and	Summer/															
1965-1995	Clay	Fall	58,877	157	62	4.60	0.128	0.05	37,225	73	78	4.27	0.238	0.05	Yes	11.35	<0.01
1965-1995/	Silt and	Summer/															
1996-2017	Clay	Fall	37,703	615	474	4.36	0.032	0.12	56,496	-268	154	4.65	-0.031	0.05	No	2.05	0.16
1949-1964/		Summer/															
1965-1995	Sand	Fall	3,464	86	13	2.54	0.787	0.11	604	138	8	1.76	1.198	0.13	Yes	9.64	<0.01
1965-1995/		Summer/															
1996-2017	Sand	Fall	235	62	22	1.35	1.302	0.20	1,011	46	12	1.90	0.933	0.09	Yes	7.52	<0.01
1949-1964/	Silt and	Winter/															
1965-1995	Clay	Spring	19,423	31	23	3.91	0.230	0.09	11,014	41	114	3.51	0.308	0.18	No	3.85	0.06
1965-1995/	Silt and	Winter/															
1996-2017	Clay	Spring	6,216	90	54	3.26	0.477	0.08	8,506	25	49	3.45	0.300	0.10	No	1.36	0.25
1949-1964/		Winter/															
1965-1995	Sand	Spring	2,602	60	10	2.53	0.758	0.09	790	98	22	1.94	1.073	0.18	Yes	4.80	0.04
1965-1995/		Winter/															
1996-2017	Sand	Spring	1,195	57	15	1.76	1.021	0.25	665	71	8	1.06	0.088	0.04	No	0.55	0.46

Table DR8. RESULTS OF HYDRAULIC MODELING

Model Run	Change in Peak Discharge (m^3/s)	% Change in Peak Discharge	Travel Time of Flood Peak (hrs)
1	5.2	2.4	6.0
2	7.9	3.7	10.5
3	9.8	4.6	12.8
4	36.6	17.2	30.5